A SOC-feedback Control Scheme for Fast Frequency Support with Hybrid Battery/Supercapacitor Storage System

Sergio Bruno
DEI - Politecnico di Bari
Bari, Italy
sergio.bruno@poliba.it

Giovanni De Carne
Institute for Technical Physics
Karlsruhe Institute of Technology
Karlsruhe, Germany
giovanni.carne@kit.edu

Cosimo Iurlaro
DEI - Politecnico di Bari
Bari, Italy
cosimo.iurlaro@poliba.it

Carmine Rodio
DEI - Politecnico di Bari
Bari, Italy
carmine.rodio@poliba.it

Mino Specchio
DEI - Politecnico di Bari
Bari, Italy
m.specchio@studenti.poliba.it

***Abstract*—Providing fast frequency regulation by means of energy storage systems is currently considered as a viable solution to low-inertia issues, caused by power electronics-interfaced generators. In particular, hybrid energy storage systems, composed by more energy storage technologies having different power and energy ratings, can optimally support the frequency regulation. A supercapacitor/battery storage system, for example, can exploit the supercapacitor dynamic active power response for synthetic inertia control, while the battery can provide primary and secondary frequency regulation. However, the optimal energy management of hybrid energy storage systems during transients needs to be addressed further in literature. In this paper, a State of Charge (SOC) feedback control scheme is proposed, that adjusts the active power output reference depending on the state of charge, avoiding excessive stress on the components and limiting the state of charge excursions. Control system parameters are optimally tuned minimizing a weighted multi-objective function in the solution of an optimal control problem. Test results adopting different weights are presented and discussed.**

***Index Terms*—Synthetic inertia, fast frequency response, frequency regulation, SOC-feedback method, hybrid energy storage system, optimal control.**

I. Introduction

With the increasing de-carbonization of energy production and the massive integration of renewable energy sources (RES), the ratio of synchronous generators connected to the power grid with respect to power electronics-based resources are dropping. As a consequence, the overall inertia of the power system is decreasing, leading to a more unstable system. Thus, frequency becomes more sensitive to load variations, which results in an increased Rate of Change of Frequency (RoCoF) and nadir following contingencies.

Several works have shown the advantages of regulating frequency through distributed energy resources, as demand response [1] or storage systems [2]–[7], adopting advanced control schemes such as synthetic inertia (SI) [2], [3], [5] or fast frequency response (FFR) [4], [5]. In [8], the authors using a single controller to provide a mixed contribution of SI and FFR, associating different weights to the proportional contributions to RoCoF and to frequency deviation.

The use of Hybrid Energy Storage Systems (HESS), consisting of integrated battery and supercapacitor, was also suggested to enhance frequency regulation. HESS can provide at the same time the high power and energy density [9]. However, it can be observed in [9], that the HESS active power demand is independent of the state of charge (SOC) of the controlled devices.

On the other hand, it is interesting to observe what is proposed by [10], where a dependency on the SOC has been introduced into the control of the BESS. Indeed, five ranges of SOC between the maximum and minimum acceptable SOC values were defined and the f-P characteristic changes depending on the range in which the SOC of BESS is located.

In [11], the frequency regulation is performed with a droop controller using Multiple Energy Storage Systems (MESS) managing the SOC. This method works by checking the SOC of the single ESS before applying the new active power set-point, that will be proportional to the current SOC. In [12] frequency regulation and SI are provided without controlling the SOC, but only considering the maximum range and the initial value, being focused on managing future contingencies. In [13] the frequency regulation is dealt with just in term of SI with ESSs, hence, this kind of controller does not provide the primary control, while, similarly to [9], the SOC is controlled

The work of Dr. Bruno was supported by Regione Puglia through the Grant No. #A1C03120 within the framework of the Programme REFIN - Research for Innovation

The work of Giovanni De Carne is supported by the Helmholtz Association within the Helmholtz Young Investigator Group "Hybrid Networks" (VH-NG-1613), and under the joint initiative "Energy System Design" in the Research Field Energy.

with an adaptive control.

This paper proposes a new control scheme that is able to provide fast frequency regulation and SI with HESS, such as batteries and supercapacitors, by modifying the exchanged active power according to the state of charge. Similar studies, as the ones in [14]–[16] where a SOC feedback method (SOCFM) is discussed, adopts SOC feedback to translate the f-P characteristic of the ESS according to its state of charge. However, such methods can only be applied to schemes that control ESS active power with a frequency-proportional control law (as in primary regulation control). The SOC feedback method proposed in this work, on the other hand, is independent of the type of control with which the set-point of active power requirement to the ESS is generated, and allows to integrate other fast frequency regulation techniques, such as synthetic inertia. Furthermore, this paper aims to optimally use different storage systems that can work together to improve frequency regulation, while safeguarding their state of charge.

II. SOC-FEEDBACK METHOD FOR FAST FREQUENCY REGULATION AND OPEN-LOOP RESPONSE ANALYSIS

In the paper, a hybrid storage system consisting of a battery and a supercapacitor, each equipped with a controller for fast frequency regulation, is modelled. This controller adopts at the same time a component proportional to frequency deviation (FFR) and a component proportional to RoCoF (SI), as also proposed in [8]. In addition to FFR/SI control, for each energy storage system, a further control function is introduced to take into account SOC variations during the implementation of fast frequency regulation. Thanks to this additional control, the state of charge of energy storage systems is safeguarded during operation. Furthermore the control allows to restore SOC to a reference value at the end of the frequency event.

The working principle of the proposed SOC feedback method is similar to the one described in [14]–[16], where SOC changes result in a translation of the f-P characteristic of the primary regulation control loop (as shown in Fig. 1 for a generic BESS). However, such method is based on applying an off-set to the frequency error and cannot be applied straightforwardly to a fast frequency controller that generates both primary regulation and synthetic inertia control actions. Differently from [14]–[16], in this paper, the proposed SOC feedback control scheme is based on the application of a feedback control signal directly to the active power reference used to control the storage unit. This scheme has the advantage of being independent of the adopted fast frequency control scheme and the energy storage technology used. When applied to a single storage system, the overall control scheme can be schematized as in Fig. 2.

As shown in Fig. 2, the SOC deviation can be calculated by integrating the active power exchanged by the storage system with the power grid over time using the expression (1):

$$\Delta SOC_{BESS}(s) = \frac{1}{E_1 \cdot h}\frac{\Delta P_{BESS}(s)}{s} = \frac{1}{K_{E1}s}\Delta P_{BESS}(s) \quad (1)$$

where ΔSOC_{BESS} and ΔP_{BESS} represent the SOC deviation and the active power deviation from the initial ones, respectively; K_{E1} is a constant representing the nominal storage capacity expressed in power per second, that is given by the product of the nominal capacity (E_1) in kWh and a conversion factor ($h = 3600$) to convert hours in seconds.

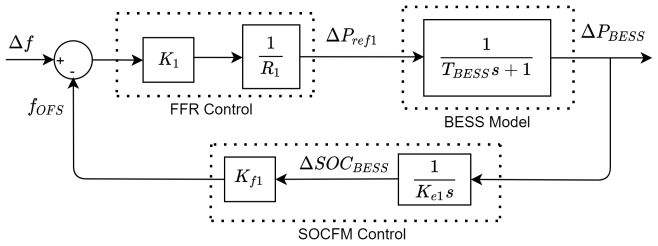

Fig. 1. SOC-feedback control scheme for primary regulation [14]–[16]

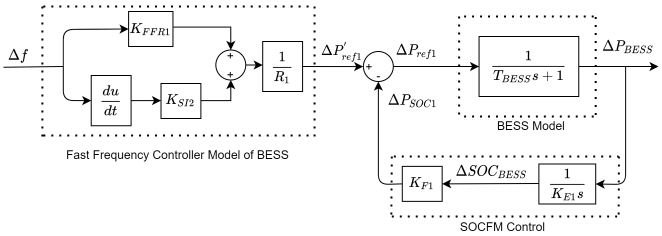

Fig. 2. Proposed SOC-feedback control scheme for fast frequency regulation

Thanks to the proposed scheme, SOC measurement is not necessary and it is possible to manage the state of charge of the energy storage system using only active power measurements. Moreveor, differently from the block-diagram in Fig. 1, where the constant K_F allows to obtain an off-set frequency correction from SOC variation, the proposed SOC-feedback method applies a correction to the reference active power output:

$$\Delta P_{SOC1}(s) = K_{F1} \cdot \Delta SOC_{BESS}(s) \quad (2)$$

In such a way, this control limits the active power required by the storage system as the SOC deviates from the initial value. The control also reestablishes the initial SOC when the control action of the fast frequency control system ceases.

In this paper, the proposed SOC-feedback method is applied to analyse the response of a hybrid energy storage system during fast regulation actions. The hybrid system consists of a BESS and a SC that can be controlled separately to provide fast frequency regulation services.

The overall model of a controlled BESS/SC hybrid energy storage system is shown in Fig. 3. The dynamic response of the two energy storage systems is modeled through first-order transfer functions. The output active power (ΔP_{BESS} and ΔP_{SC}) is used to calculate the SOC variation (ΔSOC_{BESS} and ΔSOC_{SC}) and the active power reference deviation (ΔP_{SOC1} and ΔP_{SOC2}). The output active power set-point of the fast frequency controllers ($\Delta P'_{ref1}$ and $\Delta P'_{ref2}$) is the result of the sum of two contributions: the first contribution is proportional to the frequency deviation while the second contribution is proportional to the frequency derivative (RoCoF).

Coefficients K_{FFR1}, K_{SI1} and K_{FFR2}, K_{SI2}, used for the fast frequency controller of BESS and SC, permit to split the control action into two different contribution. As also proposed in [8], the sum of each pair of coefficients can be set equal to 1.

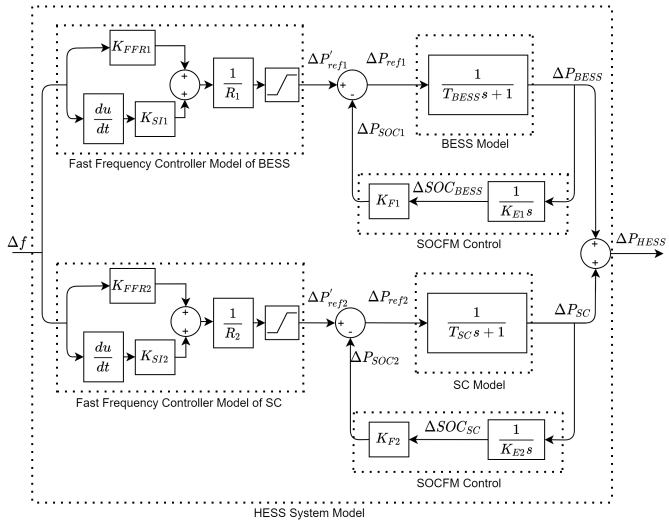

Fig. 3. Proposed SOC-feedback control scheme applied to a Hybrid Energy Storage System

III. Open-loop test of the proposed controller

The response of the proposed control scheme was tested using as input of the model in 3 the frequency transient experienced during a real severe contingency. The transient used in this test, represented in Fig. 4 was reconstructed from the frequency trend described in [17]. In this test all parameters were set as in Table I.

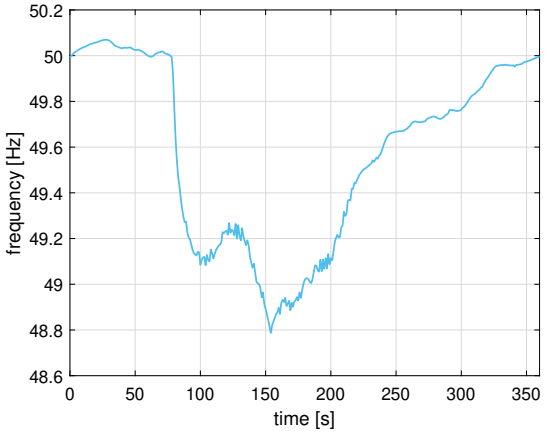

Fig. 4. Frequency transient experienced during the Aug. 9th 2019 Great Britain power system disruption event

The rated active power of each energy storage system was assumed to be 0.05 p.u. of the entire power grid. The rated active represents also the maximum active power deviation for both devices ($\Delta P^{max}_{SOC1} = \Delta P^{max}_{SOC2} = 0.05$). The energy capacity of BESS and SC, was set so that, starting from a 100% SOC, the devices can fully discharge at the rated active power in one hour and one minute, respectively. Coefficients K_{E1} and K_{E2} can be calculated according to (1).

TABLE I
System parameters

R_1	T_{BESS}	K_{E1}	K_{FFR1}	K_{SI1}	K_{F1}
0.05	0.1	180	0.8	0.2	0.167

R_2	T_{SC}	K_{E2}	K_{FFR2}	K_{SI2}	K_{F2}
0.05	0.04	3	0.2	0.8	0.1

A maximum ΔSOC^{max}_{BESS} deviation of 30% has been assumed for the BESS, whereas a ΔSOC^{max}_{SC} of 50% was considered for the SC. According to (2), coefficients K_{F1} and K_{F2} have been chosen in such way that the maximum power rate corresponds to the maximum SOC deviation.

The active power references exiting the fast-frequency controllers, $\Delta P'_{ref1}$ and $\Delta P'_{ref2}$), are limited by ΔPr^{max}_{BESS} and ΔPr^{max}_{SC}, respectively. This limit is represented by a saturation block and is necessary because the power reference actually sent to the device (ΔP_{ref1} and ΔP_{ref2}), given by the difference between the power reference arriving from the fast-frequency controller and the additional active power reference, must be able to reach zero when the SOC of the component has reached the assumed minimum or maximum SOC deviation.

Given the higher energy capacity, a greater weight has been set to the contribution proportional to the frequency deviation (higher K_{FFR1}) than the contribution proportional to the frequency derivative (lower K_{SI1}) in the fast frequency controller of the BESS. On the contrary, since the SC is a device capable of providing higher power density, a higher weight has been set in its fast frequency controller to the contribution proportional to the RoCoF (higher K_{FFR2}) than to the contribution proportional to the frequency deviation (lower K_{SI2}).

In Figs. 5 and 6 are shown the active power response and SOC behaviour of the two controlled energy storage devices for the frequency event in Fig. 4. As it can be observed in Fig. 5, for the BESS fast frequency regulator, the proportional contribution to the frequency deviation is preponderant over the proportional contribution to the frequency derivative. For this reason, a noticeable active power absorption of the BESS can be observed in the moments before the failure where a slight over-frequency was detected. On the other hand, the supercapacitor fast frequency regulator generates a SI contribution preponderant with respect to the FFR. SC behavior is slightly affected by the absolute frequency value, where as it is heavily affected by fast frequency changes and RoCoF.

The SOC responses are shown in Fig. 6. The BESS, endowed with a much larger capacity than the SC, varies its SOC only slightly during the transient. In this case the SOC feedback control does not affect significantly the BESS response. On the contrary, the SOC of the SC varies considerably and, for this reason, the active power contribution is limited in the interval from about $t = 80s$ to $t = 200s$, as it can be

observed in Fig. 5. The effect of the SOC feedback method on the active power reference sent to BESS and SC is more explicitly recognizable in Figs. 7 and 8, where it is possible to separate the frequency regulation from the SOCFM correction.

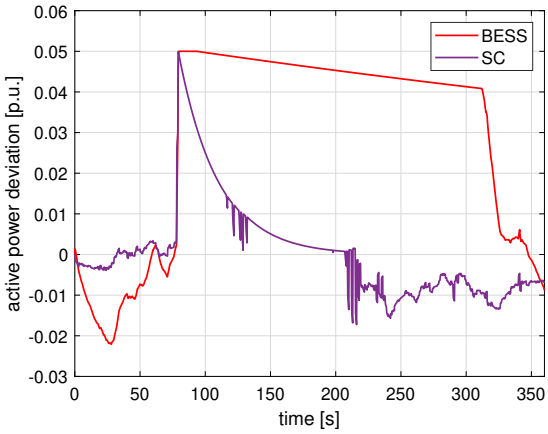

Fig. 5. Active power responses of the HESS model for open-loop response analysis

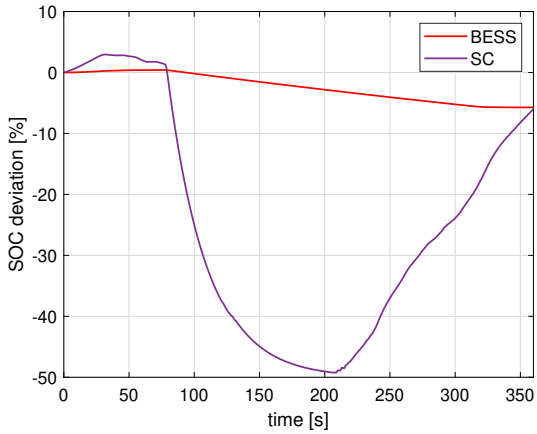

Fig. 6. SOC behaviours of the HESS model for open-loop response analysis

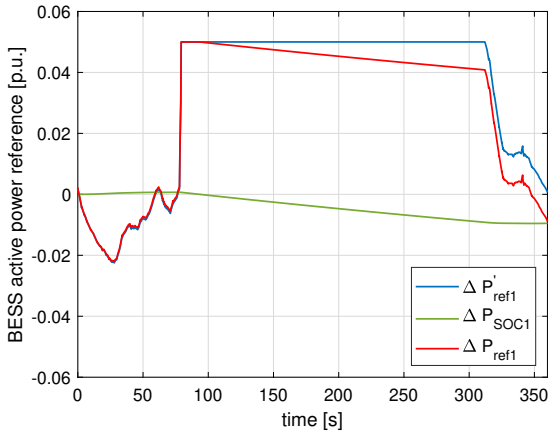

Fig. 7. BESS active power references for open-loop response analysis

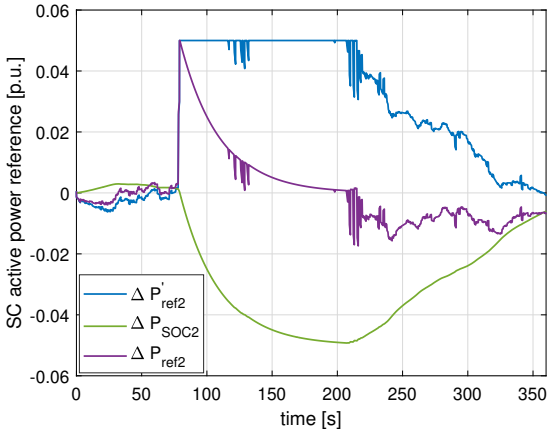

Fig. 8. SC active power references for open-loop response analysis

IV. Closed-Loop Response Analysis and Controller Parameters Optimal Tuning

In order to test the aforementioned control system performance, further simulation tests have been carried out. These simulations are aimed to study the behavior of the overall power system with additional frequency support provided by HESS. An aggregated hybrid storage system, that includes batteries and supercapacitors, has been integrated in the power system model, to provide fast frequency regulation. The overall model used is shown in Fig. 9.

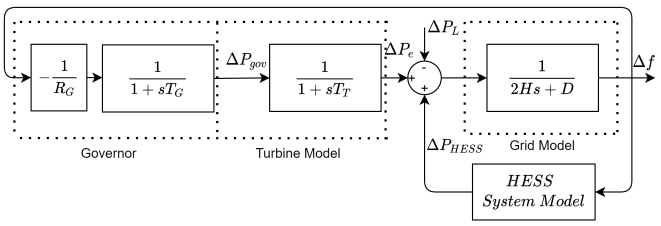

Fig. 9. Power system model with hybrid storage connected

In all tests, the system parameters were set as follows: generator droop $R_G = 5\%$, generator time constant $T_G = 0.2s$, turbine time constant $T_T = 0.3s$, total system inertia $H = 2.5s$, dumping factor $D = 2\%$.

The coefficients considered in the model have been initially chosen following the existing literature approaches [8], [16], and from the operating conditions of the devices assumed in the model. However, the gain coefficients of the fast frequency controllers (K_{FFR1}, K_{SI1}, K_{FFR2}, K_{SI2}) and the gains K_{F1} and K_{F2} can be optimally tuned by means of a generic optimization algorithm. The problem to be solved minimized a generically nonlinear function of all system variables

$$\min_{\boldsymbol{u}} \int^{T} f(\boldsymbol{x}(t), \boldsymbol{u}, d) \cdot dt \tag{3}$$

subject to the differential set of equations

$$\mathbf{h}(\boldsymbol{x}(t), \boldsymbol{u}, d) = 0 \tag{4}$$

that can be expressed in the form

$$\dot{\boldsymbol{x}} = A(\boldsymbol{u}) \cdot \boldsymbol{x}(t) + B(\boldsymbol{u}) \cdot d \tag{5}$$

$$\begin{aligned} \boldsymbol{x} &\in \boldsymbol{X} \\ \boldsymbol{u} &\in \boldsymbol{U} \end{aligned} \tag{6}$$

where

$$\boldsymbol{u}^T = [K_{FFR1}, K_{SI1}, K_{FFR2}, K_{SI2}, K_{F1}, K_{F2}] \tag{7}$$

$$\begin{aligned} \boldsymbol{x}^T = [&\Delta P_e(t), \Delta f(t), \Delta P_{gov}(t), \Delta P_{BESS}(t), \\ &\Delta P_{SC}(t), \Delta SOC_{BESS}(t), \Delta SOC_{SC}(t)] \end{aligned} \tag{8}$$

and where d represents the disturbance ΔP_L applied at $t = 0$, $\boldsymbol{X}$ takes into account all physical constraints and $\boldsymbol{U}$ limits the control variables. In (8), ΔP_{gov} and ΔP_e represent the active power variation output from the governor and turbine model blocks, respectively. Δf represents the change in frequency output from the power grid, ΔP_{BESS} and ΔP_{SC} are respectively the changes in active power output from the BESS and SC, and ΔSOC_{BESS} and ΔSOC_{SC} represent the respective changes in SOC.

Through discretization the dynamic problem formulated by eq. (3)-(8) can be converted into a static nonlinear problem in the discrete time domain:

$$\min_{\boldsymbol{u}} F(\hat{\boldsymbol{x}}, \boldsymbol{u}, d) \tag{9}$$

subject to

$$\mathbf{H}(\hat{\boldsymbol{x}}, \boldsymbol{u}, d) = 0 \tag{10}$$

$$\begin{aligned} \hat{\boldsymbol{x}} &\in \boldsymbol{X} \\ \boldsymbol{u} &\in \boldsymbol{U} \end{aligned} \tag{11}$$

$$\hat{\boldsymbol{x}}^T = [\hat{\boldsymbol{x}}_1^T,\ \hat{\boldsymbol{x}}_2^T,\ ...,\ \hat{\boldsymbol{x}}_{nstep}^T] \tag{12}$$

$$\begin{aligned} \hat{\boldsymbol{x}}_k^T = [&\Delta P_e^k, \Delta f^k, \Delta P_{gov}^k, \Delta P_{BESS}^k, \\ &\Delta P_{SC}^k, \Delta SOC_{BESS}^k, \Delta SOC_{SC}^k] \end{aligned} \tag{13}$$

where $\mathbf{H}$ is the set of discretized differential equations, $\hat{\boldsymbol{x}}_k$ represents the state variables at the k_{th} time step and $\hat{\boldsymbol{x}}$ is the state variables' simulated trajectory. The multi-objective optimization problem given by (9)-(13) is a nonlinear problem due to the combination of $\mathbf{u}$ and $\hat{\boldsymbol{x}}$ in (10) and the effect of saturation blocks in (11). However, the problem can be easily solved through any meta-heuristic method or through dynamic programming. In this paper, a Genetic Algorithm (GA) method, where each particle in the population is represented by a vector with six real components in (7), is used to solve the problem. The function *F* is a multi-objective function given by a weighted sum of six different objective functions. The suggested multi-objective function that has been employed to reach the desired performance is:

$$F(\hat{\boldsymbol{x}}, \boldsymbol{u}, d) = \sum_{i=1}^{6} \alpha_i J_i(\hat{\boldsymbol{x}}, \boldsymbol{u}, d) \tag{14}$$

The six observable objective functions in (14) have been made explicit in eq. (15)-(20). The objective functions have been normalized to have comparable values.

$$J_1 = \frac{1}{nstep} \cdot \sum_{k=1}^{nstep} \left(\frac{f^k - f^{k-1}}{f_n} \right)^2 \tag{15}$$

$$J_2 = \left(\frac{max|f^k - f_n|}{f_n} \right)^2 \tag{16}$$

$$J_3 = \frac{1}{nstep} \cdot \sum_{k=1}^{nstep} \left(\frac{P_{BESS}^k \cdot \Delta t}{E_{BESS}} \right)^2 \tag{17}$$

$$J_4 = \frac{1}{nstep} \cdot \sum_{k=1}^{nstep} \left(\frac{P_{SC}^k \cdot \Delta t}{E_{SC}} \right)^2 \tag{18}$$

$$J_5 = \frac{1}{nstep} \cdot \sum_{k=1}^{nstep} \left(\frac{P_{BESS}^k - P_{BESS}^{k-1}}{P_{BESS}^{max}} \right)^2 \tag{19}$$

$$J_6 = \frac{1}{nstep} \cdot \sum_{k=1}^{nstep} \left(\frac{P_{SC}^k - P_{SC}^{k-1}}{P_{SC}^{max}} \right)^2 \tag{20}$$

where f^k represents the system frequency at the k_{th} time step, f_n represents the nominal system frequency, P_{BESS}^k, E_{BESS} and P_{SC}^k, E_{SC} represent the active power output at the k_{th} time step and the energy capacity of the BESS and the SC, respectively. Δt is the size of the adopted time step and $nstep$ is the number of time steps into which the optimization window has been divided. In this case, a time window of 5 seconds and a time step Δt of 0.002 s have been chosen, obtaining a $nstep$ of 2500. P_{BESS}^{max} and P_{SC}^{max} represent the maximum active power output of the BESS and the SC, respectively.

Eq. (15) minimizes the sum of the frequency variations for each time step, while eq. (16) minimizes the maximum deviation of the frequency from the initial value (i.e. the nadir). These two functions are aimed to improve the system transient behaviour.

Eq. (17) and eq. (18) take into account the energy provided by the components, BESS and SC, in relation to their maximum capacity. These equations takes into account the component wear cost, in relation to the energy throughput. Eq. (19) and eq. (20) minimize the sum of the active power variations delivered by the BESS and SC, respectively. Therefore, these functions allow during the optimization, to dampen the active power variation dynamic required from the batteries, reducing the stress to the component.

The cases studied and shown below are aimed to optimize the response of the system in Fig. 9 following at a load step

variation ΔP_L of $0.1\,p.u.$ This load step was chosen equal to the the available HESS flexibility ($0.05 + 0.05\,p.u.$), in other to better observe the effects of the optimization on the HESS response. However, in actual operation the optimization could be calculated on-line with respect to updated dynamic parameters (for example a new estimate of the power system total inertia) and to an assumed worst possible contingency (for example the loss of the highest generation unit or the sudden disconnection of the highest load).

Although the functions (15)-(20) were normalized, the weights α can be chosen in such way to emphasize a specific target. For example, during alert or vulnerable conditions (for example when inertia is below a specific security threshold), components' safe keeping can be sacrificed with respect to power system security. The effects of these choices are presented in the test results. Desirable settings of weights can be obtained through extensive off-line simulations.

A. Case 1

In Case 1, the weight α_1 was set relatively high ($\alpha_1 \gg 1$), in order to induce the optimization algorithm to choose a set of the parameters $\boldsymbol{u}$ such that the RoCoF is reduced as much as possible. All other weights have been set to 1. The coefficients set $\boldsymbol{u}$, resulting from the optimization, is given in (21).

$$\boldsymbol{u}^T = [0.463, 0.537, 0.084, 0.916, 0.171, 0.100] \qquad (21)$$

In Fig. 10 the frequency behavior in the first seconds after the step load change can be observed and compared to the case with the non-optimized parameters (i.e. the values in Table I), and the case without the HESS contribution. In any case, the contribution provided by the HESS allows a clear improvement in the frequency response of the system. Compared to the non-optimized case, adopting the optimized set $\boldsymbol{u}$ in (21), the frequency reaches a larger frequency nadir but has a reduced RoCoF. In Fig. 11 and Fig. 12, it can be observed that the active power provided by the BESS during the transient is lower than in the non-optimized case, so that the stress on the component is reduced. On the other hand, similarly to the non-optimized case, the SC power capability is exploited at the rated value ($0.05p.u.$) in the very first instants following the disturbance, when maximum RoCoF is experienced. Shortly after this maximum, when the nadir is approached, the SC active power contribution rapidly decreases.

The state of charge of BESS and SC drops only slightly as it can be observed in Figs. 13 and 14. The effect of the SOCFM is therefore only slightly noticeable in the represented time window (first 10 seconds) that shows the response of primary regulation. However, if the storage power capacity is exploited for a longer period, for example also during secondary regulation, the SOCFM control can smoothly reduce the contribution required by the storage resources, avoiding a sudden triggering of storage SOC-based protections.

B. Case 2

In this second case, a higher importance is given to preserve BESS lifetime by avoiding fast active power variations. Stress

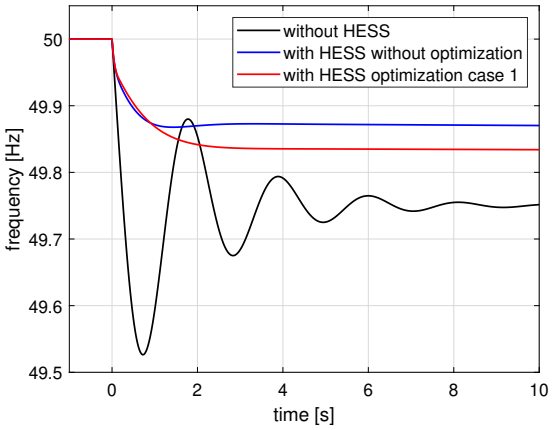

Fig. 10. Frequency behaviour with RoCoF optimization

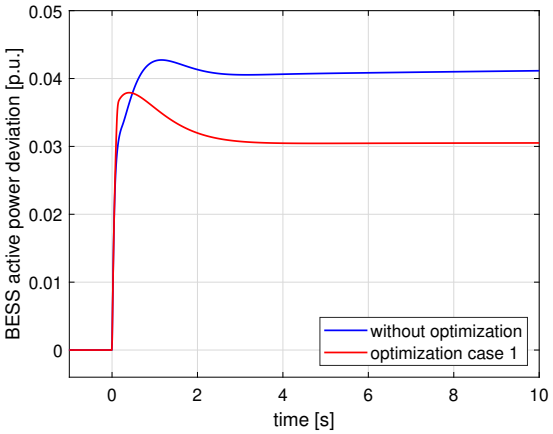

Fig. 11. Battery active power response with RoCoF optimization

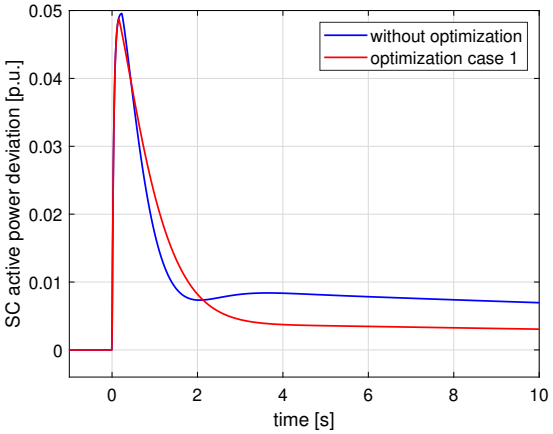

Fig. 12. Supercapacitor active power response with RoCoF optimization

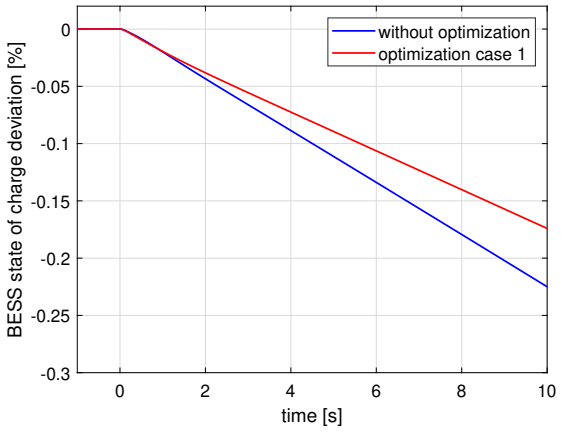

Fig. 13. Battery SOC behaviour with RoCoF optimization

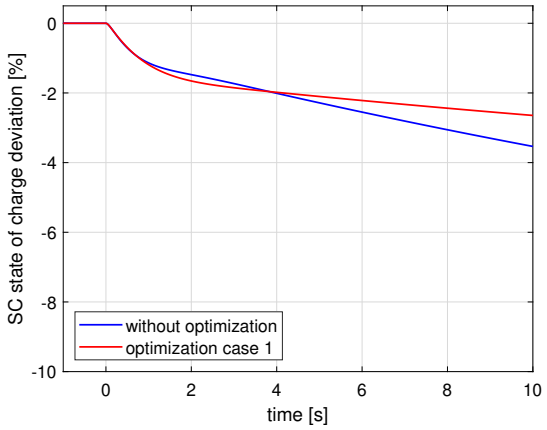

Fig. 14. Supercapacitor SOC behaviour with RoCoF optimization

on the battery was limited reducing the weight of function J_5. In this test a $\alpha_5 \gg 1$ was considered. All other weight were set to 1, obtaining the new solution

$$\boldsymbol{u}^T = [0.931, 0.068, 0.742, 0.258, 0.829, 0.101] \qquad (22)$$

By assigning a higher weight to J_5, the algorithm selected $\boldsymbol{u}$ in such a way to reduce the variations in the active power delivered by the BESS without trying to severely constrain the RoCoF. Indeed, it can be observed in Fig. 15, the RoCoF is less contained compared to the non-optimized case. On the other hand, the frequency nadir is more contained. The reason can be observed in Figs. 16, where it is shown how the BESS provide less active power than the optimized Case 1 in the first instants after the contingency, but provide more active power during the remaining part of the transition. Similarly, also the power contribution provided by the SC after the nadir is higher than in case 1 and the non-optimized case.

This effect is due to the higher values of K_{FFR1} and K_{FFR2} resulting from this second optimization. These high values of K_{FFR1} and K_{FFR2} are obtained because the weight assigned to function J_1 is no longer predominant with respect to the others. This condition gives a higher nadir but faster component discharge in cases where the frequency remains at a value other than the reference value after the disturbance. Indeed, it can be seen from Figs. 18 and 19 how the SOC of the two components decreases more than in Case 1.

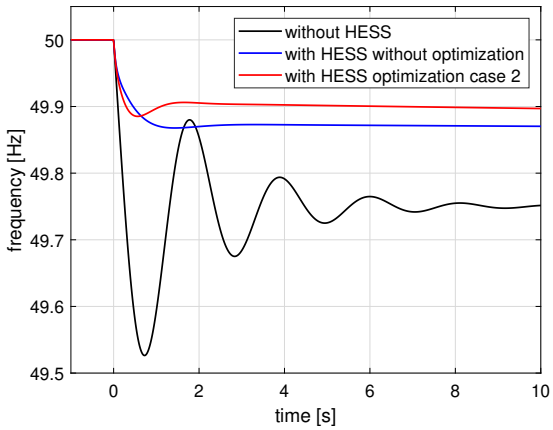

Fig. 15. Frequency behaviour with battery response optimization

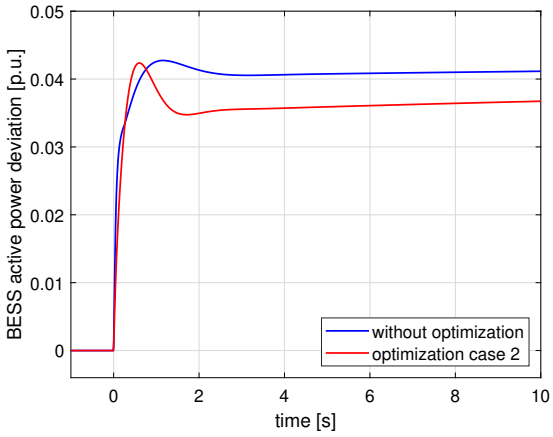

Fig. 16. Battery active power response with battery response optimization

V. Conclusions

This paper presented a study aiming to demonstrate how hybrid energy storage systems, composed by supercapacitor and battery, can be exploited to improve power system frequency response. The HESS control scheme for fast frequency regulation is updated with a SOC control of the devices to prevent sudden reductions in the state of charge and return the device charge to the pre-disturbance condition after the transient. It has been shown how, through targeted optimization of control parameters, it is possible to derive controller parameters in order to achieve an improvement in frequency response and/or avoid excessive component stress. The results demonstrate how giving more weight to battery protection rather than reducing RoCoF during a disturbance visibly changes the frequency behaviour. Furthermore, the SOC control permits

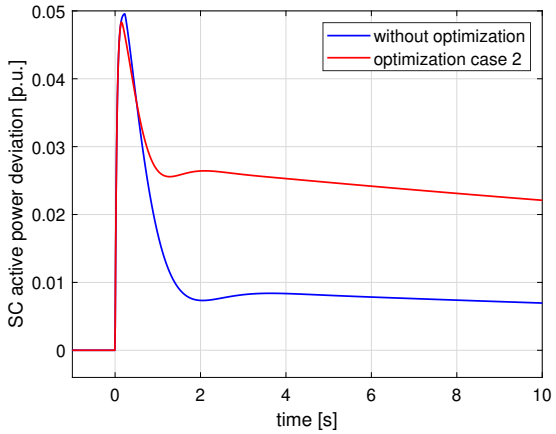

Fig. 17. Supercapacitor active power response with battery response optimization

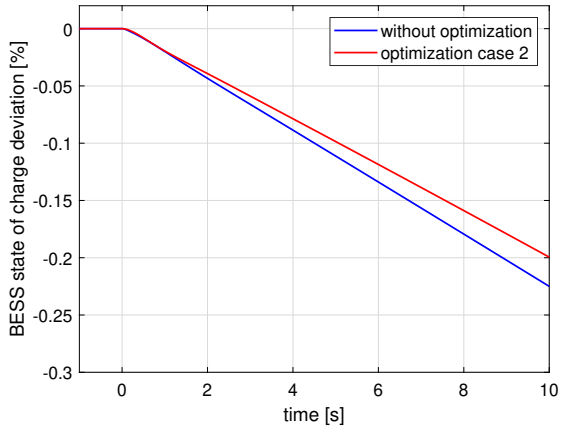

Fig. 18. Battery SOC behaviour with battery response optimization

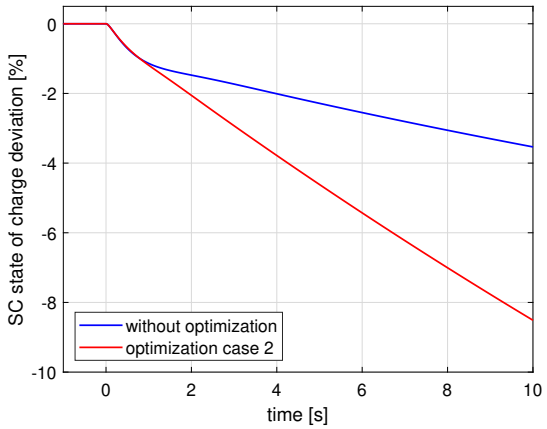

Fig. 19. Supercapacitor SOC behaviour with battery response optimization

safeguarding of the state of charge without limiting the action of the components during frequency transients.

REFERENCES

[1] S. Bruno, G. Giannoccaro, C. Iurlaro, M. L. Scala, C. Rodio, and R. Sbrizzai, "Fast Frequency Regulation Support by LED Street Lighting Control," pp. 1–6, 2021.

[2] S. Bruno, G. Giannoccaro, C. Iurlaro, M. L. Scala, and C. Rodio, "A Low-cost Controller to Enable Synthetic Inertia Response of Distributed Energy Resources," in *2020 IEEE EEEIC/I&CPS Europe*, 2020, pp. 1–6.

[3] R. Zhang, J. Fang, and Y. Tang, "Inertia emulation through supercapacitor energy storage systems," in *2019 10th International Conference on Power Electronics and ECCE Asia (ICPE 2019 - ECCE Asia)*, 2019, pp. 1365–1370.

[4] J. Kim, V. Gevorgian, Y. Luo, M. Mohanpurkar, V. Koritarov, R. Hovsapian, and E. Muljadi, "Supercapacitor to provide ancillary services with control coordination," *IEEE Transactions on Industry Applications*, vol. 55, no. 5, pp. 5119–5127, 2019.

[5] J. A. Adu, J. D. Rios Penaloza, F. Napolitano, and F. Tossani, "Virtual inertia in a microgrid with renewable generation and a battery energy storage system in islanding transition," in *2019 1st International Conference on Energy Transition in the Mediterranean Area (SyNERGY MED)*, 2019, pp. 1–5.

[6] S. Karrari, H. R. Baghaee, G. De Carne, M. Noe, and J. Geisbuesch, "Adaptive Inertia Emulation Control for High-speed Flywheel Energy Storage Systems," *IET Generation, Transmission & Distribution*, vol. 14, no. 22, pp. 5047–5059, 2020.

[7] S. Karrari, G. De Carne, and M. Noe, "Model validation of a high-speed flywheel energy storage system using power hardware-in-the-loop testing," *Journal of Energy Storage*, vol. 43, p. 103177, 2021.

[8] L. Toma, M. Sanduleac, S. A. Baltac, F. Arrigo, A. Mazza, E. Bompard, A. Musa, and A. Monti, "On the virtual inertia provision by bess in low inertia power systems," in *2018 IEEE International Energy Conference (ENERGYCON)*, 2018, pp. 1–6.

[9] U. Akram and M. Khalid, "A coordinated frequency regulation framework based on hybrid battery-ultracapacitor energy storage technologies," *IEEE Access*, vol. 6, pp. 7310–7320, 2018.

[10] S. Sitompul and G. Fujita, "Implementation of bess load frequency control in islanded microgrid system by considering soc," in *2020 IEEE PES Innovative Smart Grid Technologies Europe (ISGT-Europe)*, 2020, pp. 980–984.

[11] J. W. Shim, G. Verbič, K. An, J. H. Lee, and K. Hur, "Decentralized operation of multiple energy storage systems: Soc management for frequency regulation," in *2016 IEEE International Conference on Power System Technology (POWERCON)*, 2016, pp. 1–5.

[12] V. Knap, S. K. Chaudhary, D.-I. Stroe, M. Swierczynski, B.-I. Craciun, and R. Teodorescu, "Sizing of an energy storage system for grid inertial response and primary frequency reserve," *IEEE Transactions on Power Systems*, vol. 31, no. 5, pp. 3447–3456, 2016.

[13] M. F. Silva, G. C. Guimarães, F. A. M. Moura, D. B. Rodrigues, A. C. Souza, and L. R. C. Silva, "System frequency support by synthetic inertia control via bess," in *2019 IEEE PES Innovative Smart Grid Technologies Conference - Latin America (ISGT Latin America)*, 2019, pp. 1–6.

[14] T.-A. Nguyen-Huu, V. T. Nguyen, K. Hur, and J. W. Shim, "Coordinated control of a hybrid energy storage system for improving the capability of frequency regulation and state-of-charge management," *Energies*, vol. 13, no. 23, 2020. [Online]. Available: https://www.mdpi.com/1996-1073/13/23/6304

[15] J. W. Shim, G. Verbič, N. Zhang, and K. Hur, "Harmonious integration of faster-acting energy storage systems into frequency control reserves in power grid with high renewable generation," *IEEE Transactions on Power Systems*, vol. 33, no. 6, pp. 6193–6205, 2018.

[16] J. W. Shim, G. Verbič, H. Kim, and K. Hur, "On droop control of energy-constrained battery energy storage systems for grid frequency regulation," *IEEE Access*, vol. 7, pp. 166 353–166 364, 2019.

[17] BEIS - Department for Business, Energy & Industrial Strategy, "GB Power System Disruption - 9 August 2019," Tech. Rep., 2019.

Karlsruher Institut für Technologie

OPEN ACCESS

Repository KITopen

Dies ist ein Postprint/begutachtetes Manuskript.

Empfohlene Zitierung:

Bruno, S.; De Carne, G.; Iurlaro, C.; Rodio, C.; Specchio, M.
A SOC-feedback Control Scheme for Fast Frequency Support with Hybrid Battery/Supercapacitor Storage System.
2021. 2021 6th IEEE Workshop on the Electronic Grid (eGRID), Institute of Electrical and Electronics Engineers (IEEE).
doi:10.5445/IR/1000141661

Zitierung der Originalveröffentlichung:

Bruno, S.; De Carne, G.; Iurlaro, C.; Rodio, C.; Specchio, M.
A SOC-feedback Control Scheme for Fast Frequency Support with Hybrid Battery/Supercapacitor Storage System.
2021. 2021 6th IEEE Workshop on the Electronic Grid (eGRID), 1–8, Institute of Electrical and Electronics Engineers (IEEE).
doi:10.1109/eGRID52793.2021.9662149

Lizenzinformationen: KITopen-Lizenz